Chapter 7

Effects of Cross Sectional Shape and Confining Material

The finite element (FE) model is utilized to compare the performance of square versus circular cross sections, as well as fiber reinforced polymer (FRP) versus steel hoop confined sections. A series of concrete axial stress versus strain curves are generated with different confinement levels for each confining material. An axial load-moment strength interaction diagram is created for the highest confinement level for each cross sectional shape and confining material. Using these analyses, a comparison is performed to examine how cross sectional shape and confining material affect the strength and ductility of the section. The cross sections and loading details are described in Section 7.1. The results of this comparison are discussed in Section 7.2.

This comparison can be used to highlight the different advantages and disadvantages of the different section shapes and confining materials. Designers face many decisions when laying out the details of a section. For each specific application, a slightly different performance standard may be applied. By understanding the effects of these two design variables, the designer is able to choose the shape or confining material that exhibit more optimal performance for the specific application.

7.1 Discussion of Sections Used for Performance Comparison

A square and a circular cross section, both confined by steel hoops, are designed in order to examine the effects of cross sectional shape. To more easily facilitate the comparison, the two sections are designed to have an identical confined area. It is important that the two cross sections have the same confined area because it is expected that the cover concrete will spall off and become ineffective. Details of the two cross sections are shown in Figure 7.1. For both sections, hoop spacings of 3, 6,

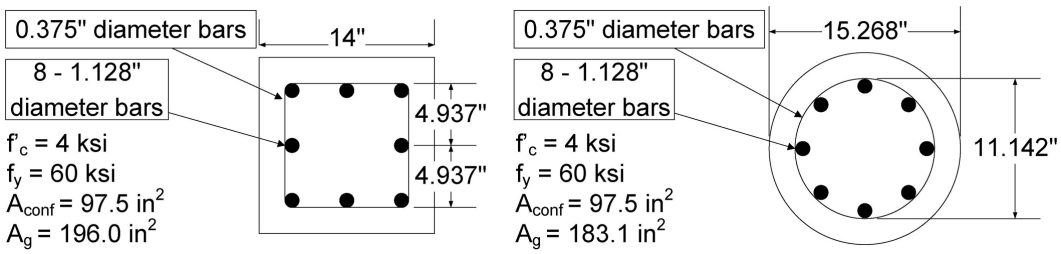

Figure 7.1: Details of square and circular cross sections confined by steel hoops.

10, and 14 inches (76, 152, 254, and 356 mm) are employed. A concrete axial stress versus strain curve is computed for each cross section and hoop spacing. The FE meshes used to represent these cross sections are shown in Appendix H. As discussed in Sections 6.2.4 and 6.2.5, it is necessary to modify the concrete model to have a round residual surface in order to predict the behavior to sufficiently large compressive strain levels. This is only necessary for axial loading of the steel confined sections. Recall that use of the round residual surface is expected to slightly overstimate the residual stress for loading which is not close to a Lode angle of 60°. All other analyses are performed with the original concrete model as described in Chapter 4. An axial load-moment interaction diagram was created for both cross sections with the 3 inch (76 mm) hoop spacing only.

A similar configuration is then considered with an alternative confining material. The steel hoops are removed from the FE model and replaced with an E-glass FRP around the outside of each section. In this configuration, the confined area is no

longer identical for the square and the circular cross sections. The confined area of the square cross section is 196.0 square inches (1265 square centimeters), whereas the confined area for the circular cross section is 183.1 square inches (1181 square centimeters). The E-glass FRP used for confinement has a strength of 428 lb per inch per ply (75 N per mm per ply) and an elastic modulus of 28 kips per inch per ply (4.9 kN per mm per ply). The FE meshes used to predict the behavior of these sections are shown in Appendix H. Concrete axial stress versus strain curves are generated for a confinement of 10 and 30 plies of the E-glass FRP. An axial load-moment interaction diagram is then generated for the two cross sections confined by 30 plies of E-glass FRP. Note that four of the axial load-moment cases required a refined mesh, shown in Figure H.5.

It is difficult to define what a comparable amount of confinement for steel hoops and E-Glass FRP is. In order to evaluate the confinement amounts for these two disparate materials, the elastic stiffness of each particular confinement configuration was evaluated. Table 7.1 shows the configuration of steel hoops that equates to the same confinement stiffness as a given ply count of E-Glass FRP.

Table 7.1: Confinement equivalence by elastic stiffness.

Number of E-Glass Plies	Equivalent Hoop Spacing (in)	Steel Hoop Bar Number	Steel Hoop Bar Area (in^2)
10	11.4	#3	0.11
10	20.7	#4	0.20
30	3.8	#3	0.11
30	6.9	#4	0.20
30	10.7	#5	0.31

7.2 Results of Comparison

The performance comparison for purely axial loads is presented in Section 7.2.1. Results of the axial load-moment interaction diagram are discussed in Section 7.2.2. In considering the performance of columns, axial load and moment capacity are the typical metrics used to determine the capability of the section to perform as required.

Thus, these quantities are used to explore the effects of section shape and confining material on the behavior of the column.

7.2.1 Axial Load Performance Comparison

As discussed in Sections 6.2.4 and 6.2.5, the analysis terminates prematurely when steel hoops are used for confinement. Thus, for the pure axial load cases of the steel confined sections only, the residual surface is round with the tensile meridian changed to match the compression meridian. For the E-glass FRP confined sections, the residual surface defined in Section 4.3 is used.

Concrete axial stress versus strain curves for the steel confined sections are shown in Figure 7.2, and for the E-glass FRP confined sections in Figure 7.3. The uncon-

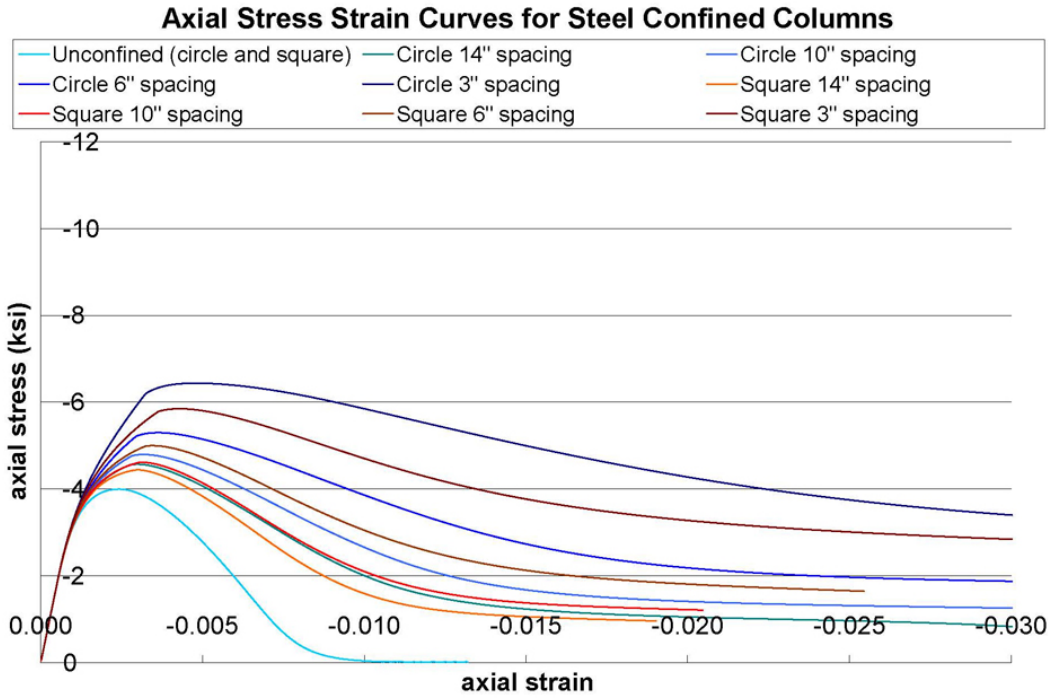

Figure 7.2: Comparison of the axial performance of steel confined sections.

fined square and circular sections have identical axial stress versus strain curves as predicted by the FE model. For the E-glass FRP confined cases, all modeled sections terminated with failure of the E-glass FRP (meaning that failure was defined by rupture of the fibers in the FRP).

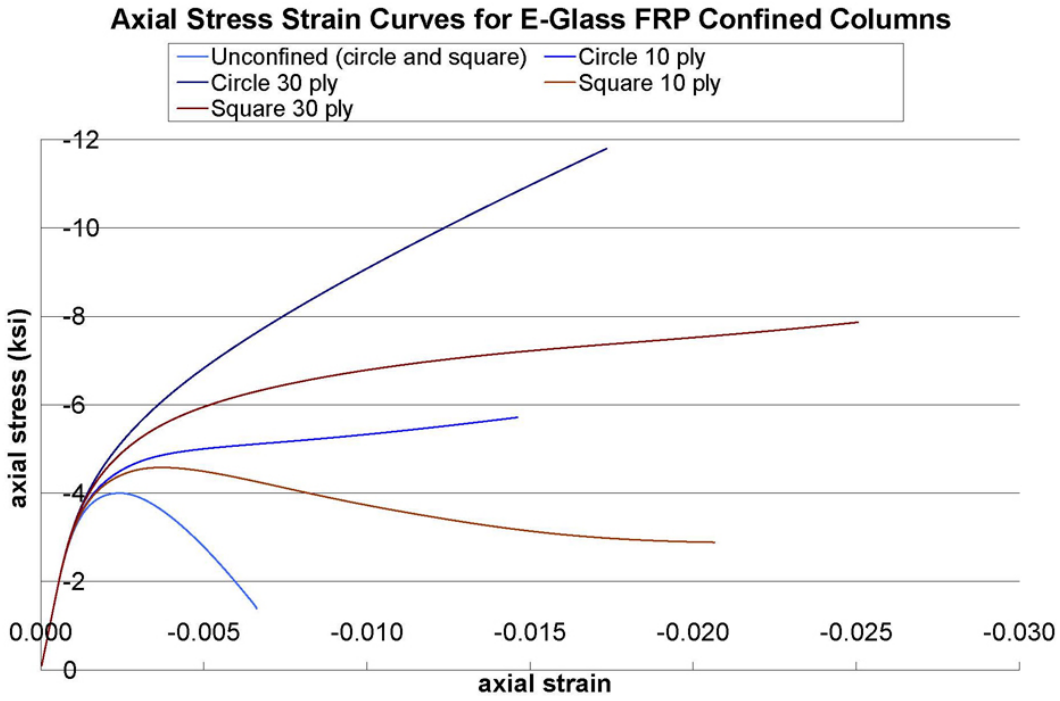

Figure 7.3: Comparison of the axial performance of E-glass confined sections.

For both types of confining materials, higher concrete stresses are supported by the circular sections than the comparable square sections, as expected due to the fact that confinement is more effective in circular sections. It is difficult to discern from Figure 7.2 how the two steel confined cross sections compare in ductility. Thus, Table 7.2 compares the strains at peak stress to those when the stress falls to 50% of the peak stress. The strain ratio is defined as the strain at 50% of peak stress divided by the strain at peak stress. It is clear that the ductility of the circular cross sections exceeds that of the square cross sections for the case of steel confinement. However, this is achieved through more effective use of the confinement, which leads to higher strains in the confining material for the circular sections (as shown by the last column of Table 7.2). The higher strains in the confinement for circular sections is more readily seen in the E-glass FRP results, since rupture of the FRP dictates the axial strain at failure. While the strength increase is much higher in the circular sections, the final axial strain of the square cross sections is higher because the FRP is not as highly stressed for this case. This lower stress in the FRP means that rupture of the FRP will occur at a higher axial strain. Thus, if a designer

Table 7.2: Strength and ductility comparison of square versus circular steel confined sections.

Cross Section Shape	Hoop Spacing (in)	Peak Stress (ksi)	Peak Stress $/f'_c$	Strain at Peak Stress	Strain at 50% of Peak Stress	Strain Ratio	Confinement Plastic Strain at 50% of Peak Stress
Circle	14	-4.574	1.143	-0.0030	-0.0092	3.084	0.0081
Circle	10	-4.799	1.200	-0.0032	-0.0109	3.404	0.0100
Circle	6	-5.302	1.326	-0.0036	-0.0155	4.270	0.0151
Circle	3	-6.441	1.610	-0.0048	-0.0341	7.079	0.0343
Square	14	-4.448	1.112	-0.0030	-0.0082	2.734	0.0054
Square	10	-4.620	1.155	-0.0031	-0.0093	3.009	0.0063
Square	6	-5.000	1.250	-0.0034	-0.0123	3.580	0.0087
Square	3	-5.851	1.463	-0.0043	-0.0274	6.405	0.0211

was concerned more about the axial strain of the section at confinement rupture, the square cross section would outperform the circular cross section. However, if the greater concern is the load carrying capacity of the column, the circular cross sections consistently outperform the square cross sections. With structural design, the designer often requires a ductile failure mode. These results raise the question of what exactly represents a ductile failure. If it is desirable that the specimens exhibit some form of softening as a warning of the onset of failure, only the square cross section confined by 10 layers of FRP would be considered to exhibit ductile failure. All other sections reach their peak stress simultaneously with the failure of the E-glass FRP. This may be considered a brittle failure mode, as the onset of failure is not preceded by softening and redistribution of the load. Examples of this brittle failure can be found in the literature (Pulido et al., 2004). However, all FRP confined sections are still reaching large strain values. Reaching large strains may also be considered ductile. The difference is that those three specimens are continuing to take load right up to the failure point, which may be a useful behavior, depending upon the individual structure being considered. This type of behavior is not typically seen in reinforced concrete members. The designer must think about what ductility means and its purpose for the individual structure being considered. Thus, when designing a section using FRP confinement, it is important to correctly design the

number of plies so that the section will exhibit the behavior desired by the designer. The FE model can be used for this purpose.

7.2.2 Axial Load-Moment Performance Comparison

No convergence problems are experienced when moments are applied to steel confined sections. Thus, the residual surface as defined in Chapter 3 is used for all FE model predictions in this section (with the exception of the steel confined pure axial load cases, as discussed in Section 7.1). The axial load-moment interaction diagrams for the two cross-sections confined by either 30 plies of E-glass FRP or steel hoops at 3 inch (76 mm) spacing are shown in Figure 7.4. For reference, ACI Committee

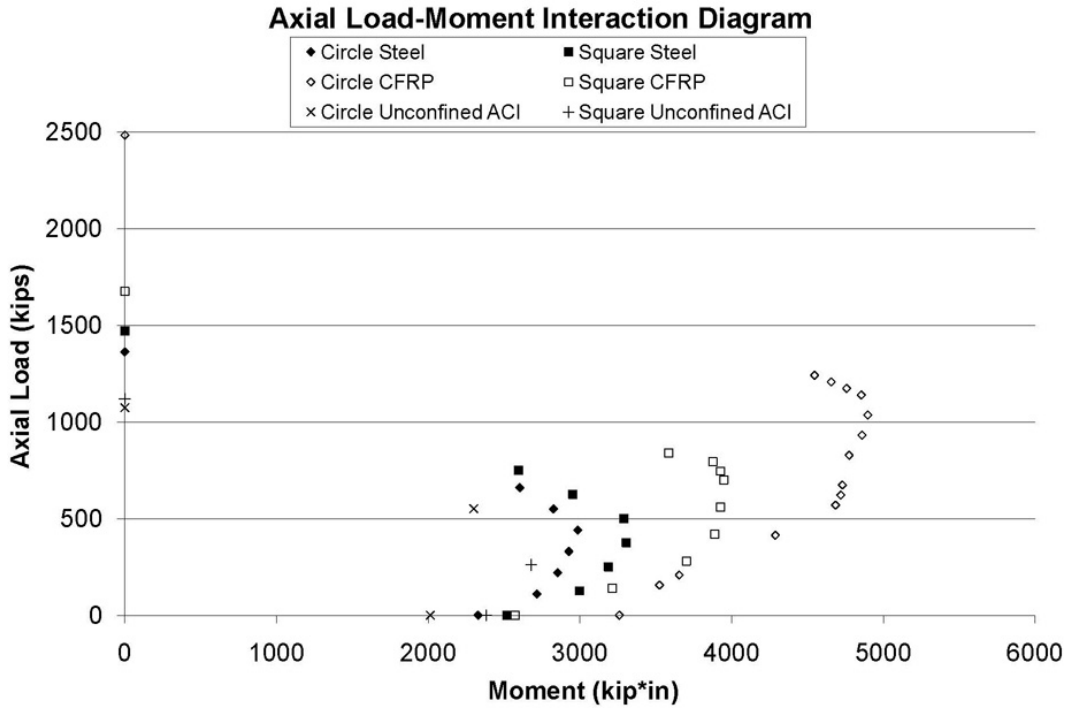

Figure 7.4: Axial load-moment interaction diagram for all four different sections.

318 (2000) equations were used with the assumption of unconfined concrete to make the predictions labeled as unconfined ACI. As with the axial loadings, the circular cross section confined by the E-glass FRP terminated with failure of the confining material. However, the square cross sections confined by E-glass FRP did not reach their peak moments at composite failure, but were instead limited by the strength

of the concrete. For the steel confined case, the square cross section withstands higher moments than the circular. This is likely due to the fact that the square cross section has a higher gross area than the circular section, and the fact that more of the area is distributed away from the neutral axis, thereby yielding a higher moment capacity. The pattern is reversed for the E-glass confined sections, with the circular cross section sustaining higher loads than the square. This is an unexpected result due to the fact that many consider confinement to be ineffective at increasing moment capacity, which may not be correct. A possible explanation is that the less effective confinement of the square section is not able to prevent degradation of the concrete, whereas in the circular section, the confinement is able to prevent the concrete from softening. Thus, confinement effectiveness comes into play with the FRP sections. This would not be the case for the steel confined sections because the concrete that is supporting the compression side of the moment couple is outside the steel hoops. For the FRP confined sections, all concrete is confined.

In order to more easily compare the increase in moment capacity with axial load, the axial load is normalized by the pure axial load capacity of the section, and the moment is normalized by the pure moment capacity of the section. This normalized axial load-moment interaction diagram is shown in Figure 7.5. For both types of confinement, the square section actually has a larger increase in moment capacity with the addition of axial load than the circular section. Since no unconfined sections were modeled, it is difficult to know if this is an effect of the shape or the effectiveness of the confinement. From Section 7.2.1, it is seen that in the case of pure axial loading, the circular sections showed a greater increase in axial load carrying capacity with confinement than the square sections. Therefore, it is likely that the square sections' outperformance of the circular sections' is due to the shape, not the effectiveness of the confinement. Clearly, the E-glass FRP shows a greater increase in moment capacity with the addition of load than the comparable steel confined section. As with pure axial loading, the E-glass FRP creates a stronger section than a comparable steel confined section. From Table 7.1, the stiffness of 30 plies of E-Glass FRP is equivalent to #3 bars at approximately 4 inch (100 mm) hoop spacing. Yet the 30 ply E-Glass

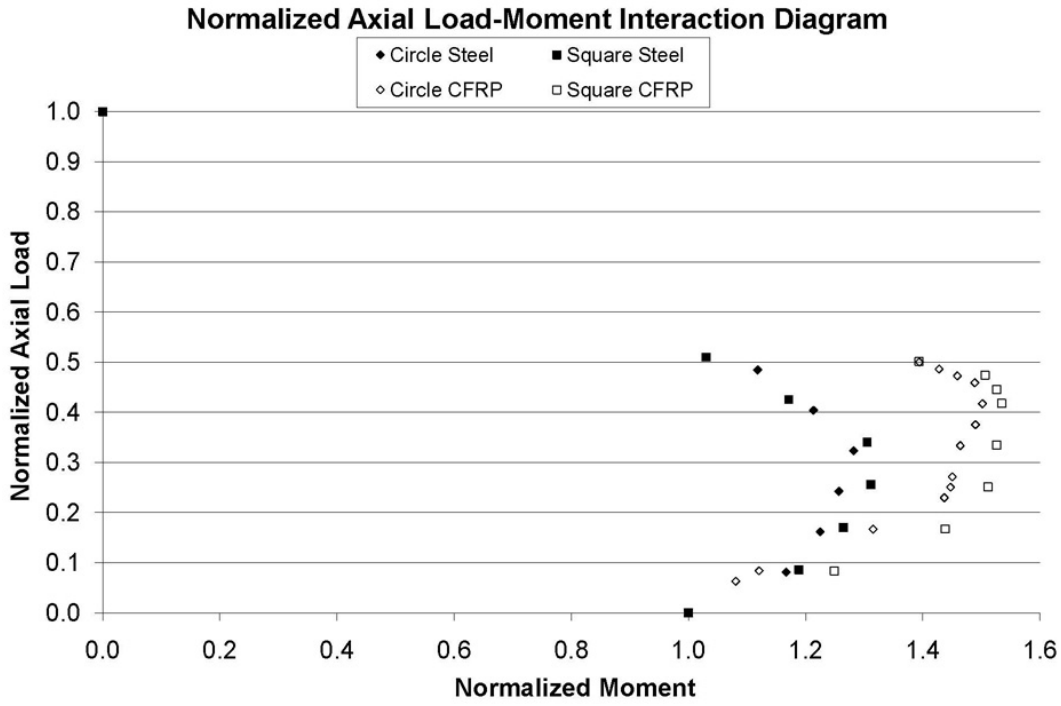

Figure 7.5: Normalized axial load-moment interaction diagram for all four different sections.

FRP confined section shows a greater increase in strength than the section confined by #3 bars at 3 inches (76 mm). However, this strength increase again comes at the cost of a loss of ductility, as will be seen in the following figures.

Figures 7.6 through 7.9 show the moment-curvature curves for all points computed for the axial load-moment interaction diagrams. Several moment-curvature curves show a small drop due to the occasional convergence problem. However, the solution always returns to the correct path. It is in these plots that the performance of the E-glass FRP confined circular section stands out. The curvature values for that section are significantly higher at failure than any other section modeled. However, as previously mentioned, failure is caused by rupture of the composite, which may not be considered a ductile failure mode. Thus, this section may not be desirable to designers seeking to create a ductile structure, depending upon that designer's definition of ductility. However, if fewer plies of the E-glass FRP were used, the section would return to a more ductile failure mode, albeit at a lower strength. This may be more useful for structural design purposes. The three other sections showed

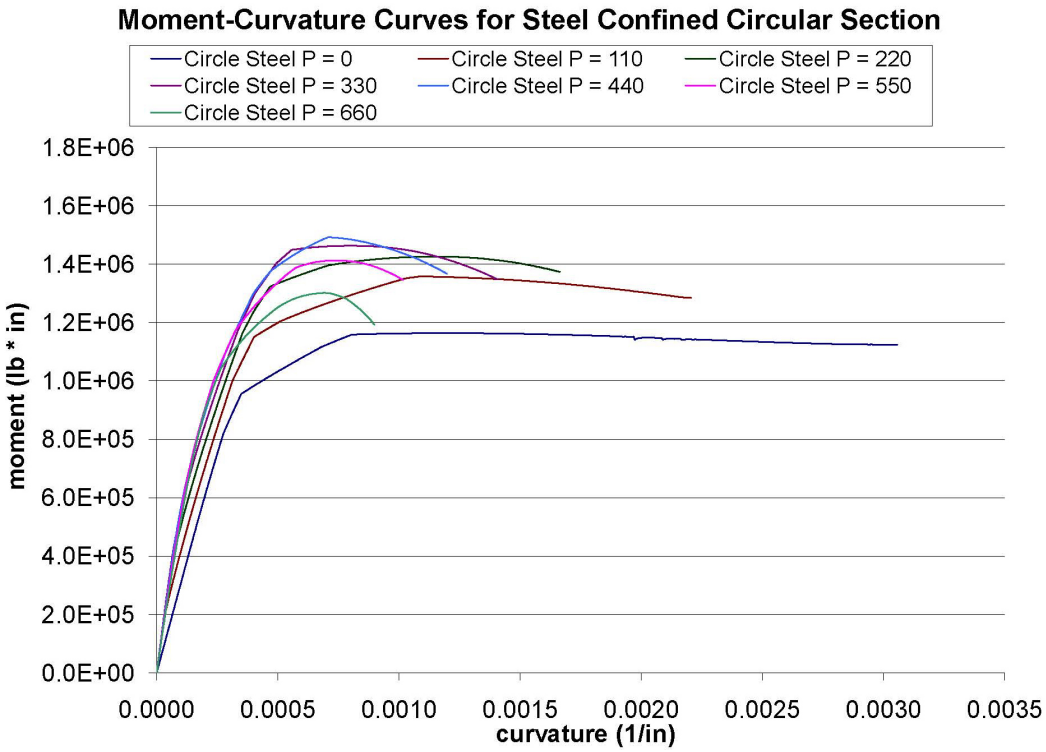

Figure 7.6: Moment versus curvature curves for the steel confined circular cross section.

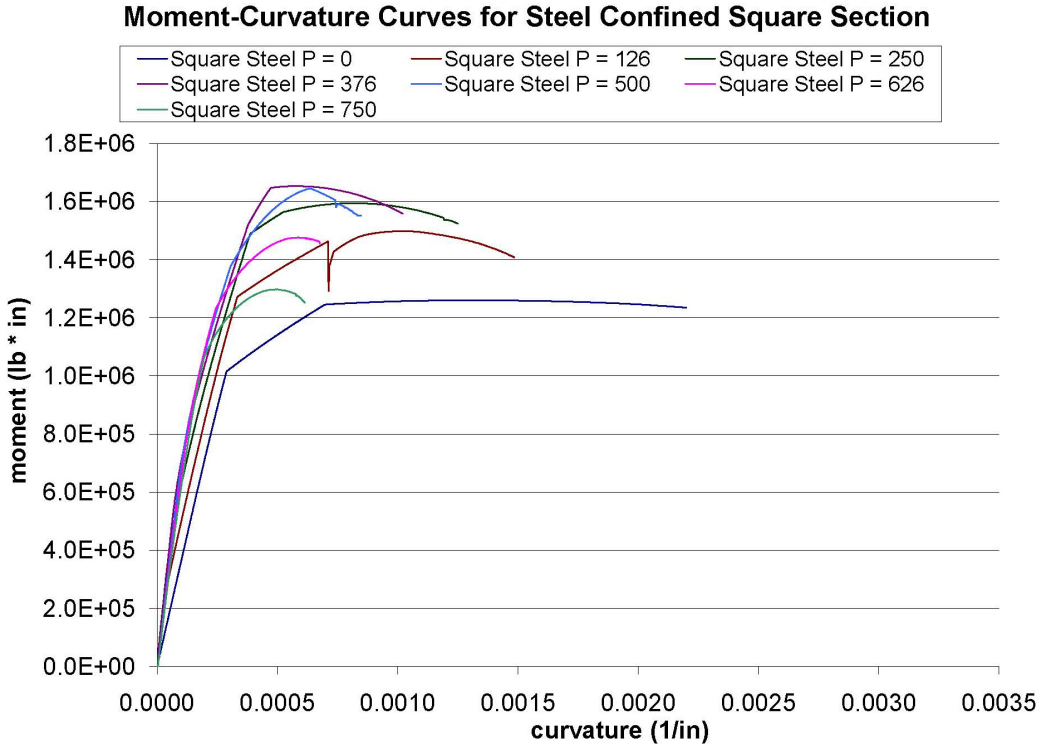

Figure 7.7: Moment versus curvature curves for the steel confined square cross section.

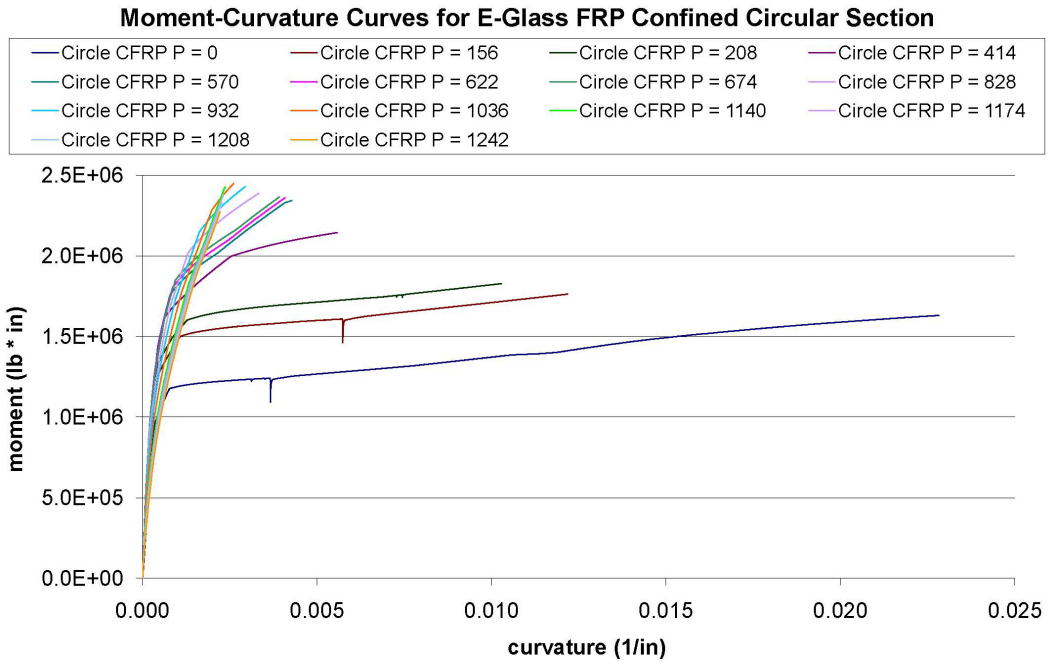

Figure 7.8: Moment versus curvature curves for the E-glass FRP confined circular cross section.

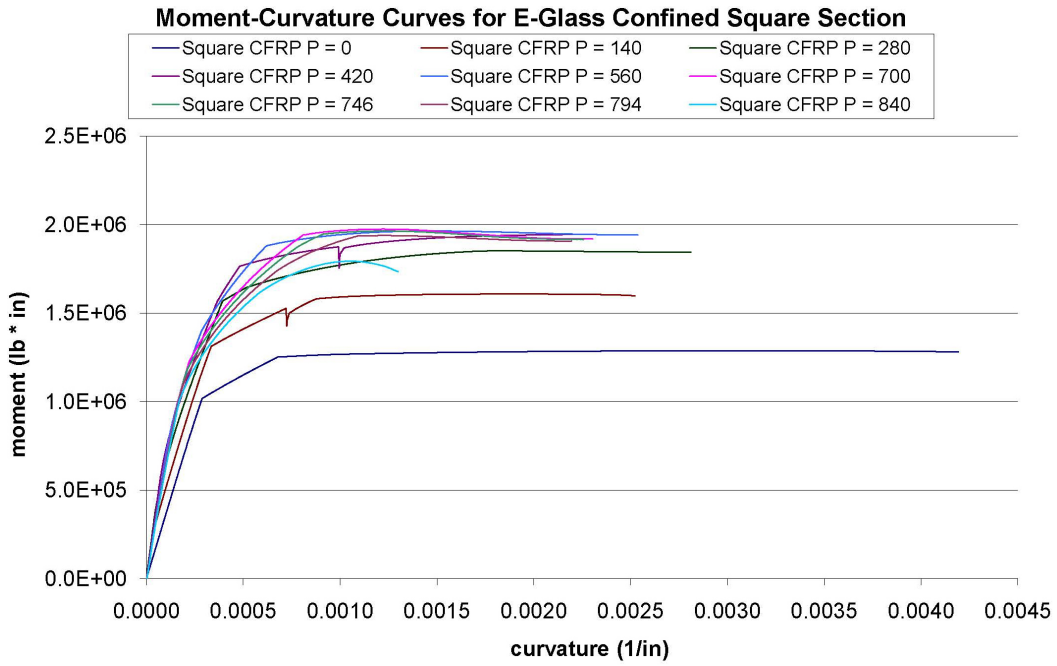

Figure 7.9: Moment versus curvature curves for the E-glass FRP confined square cross section.

somewhat less strength and significantly less curvature at failure. However, failure for the lower axial load levels was preceded by strain softening.

Clearly, when choosing the confining material and section geometry, many different factors come into play. These analyses are designed to highlight the tradeoff between strength and ductility that is seen for the FRP versus steel confinement, and for square versus circular cross sections. It is important for the designer to keep this trade off in mind when choosing the right confining material and geometry.